Progress In Electromagnetics Research, Vol. 111, 25–41, 2011

TUNABLE AND SWITCHABLE BANDPASS FILTERS USING SLOT-LINE RESONATORS

J.-X. Chen, J. Shi, and Z.-H. Bao

School of Electronics and Information, Nantong University
9 Seyuan Road, Nan Tong, Jiangsu 226019, China

Q. Xue

State Key Laboratory of Millimeter Waves
Department of Electronic Engineering, City University of Hong Kong
Tat Chee 83, Kowloon, Hong Kong SAR, China

Abstract—In this paper, novel uniplanar tunable and switchable bandpass filters are designed by using the centrally-loaded slot-line resonator. From the voltage-wave distribution along the resonator, the appropriate location for the loading element is determined to be the center of the slot-line resonator, where the voltages of the fundamental signal and second harmonic are maximum and zero, respectively. As a result, the fundamental frequency can be tuned while the second harmonic remains almost unchanged. For the first time, the properties of the centrally-loaded slot-line resonator are analyzed by using the even- and odd-mode method, and their respective resonant frequencies are derived. The demonstrated tunable bandpass filter can give a 30.9% frequency tuning range with acceptable insertion loss when a varactor is used as the loading element. By replacing the loading varactors with PIN diodes, a switchable bandpass filter is realized in which the attenuation in the fundamental passband can be controlled. In experiments, the switchable bandpass filter exhibits a 2.13 dB insertion loss in the fundamental passband when the PIN diodes are off and more than 49 dB isolation across the passband when the PIN diodes are on.

Received 8 October 2010, Accepted 5 November 2010, Scheduled 27 November 2010
Corresponding author: Zhi-Hua Bao (bao.zh@ntu.edu.cn).

1. INTRODUCTION

The reconfigurable circuits and antennas [1–5] have drawn much attention in many modern microwave/RF systems, such as the multi-band telecommunication systems, radiometers and wide-band radar systems, because of their diversity and high integration. The bandpass filter, as a key component in these systems, should also be reconfigurable to meet the system requirements. So far, many reconfigurable bandpass filters with tunability of operation frequency [6–14] and passband switching ability [15–18] have been widely developed. For the tunable filter, the use of semiconductor varactors as variable capacitors has been the most popular choice to modify the effective electrical length of the resonator and to tune the center frequency of the passband. Recently, much work has concentrated on the development of tunable bandpass filters based on microelectromechanical systems (MEMS) [12–14] due to their high quality factor Q. For the switchable bandpass filter, which has integrated a bandpass filter and a switch into single circuit, the most effective design method is to use the PIN diode to control the passband [17].

For the microstrip tunable and switchable bandpass filters [4, 17], mounting the devices in series or parallel and drilling through the substrate are inevitable. For example, in the tunable combline filter [8], the two ends of the quarter-wavelength resonator with a varactor need to be connected to ground by via. Drilling adds cost and discontinuities which make the design more difficult and degrade the performance, especially at millimetre-wave frequencies. In addition, the microstrip properties including characteristic impedance and wavelength are sensitive to the substrate thickness, which further complicates the designs at higher frequencies. To overcome these problems, the slot-line

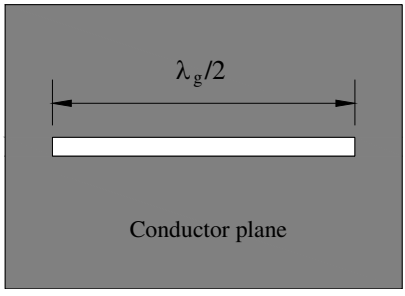

Figure 1. Slot-line half-wavelength ($\lambda_g/2$) resonator.

half-wavelength ($\lambda_g/2$) resonator [19–22] shown in Fig. 1 is investigated for the designs of tunable and switchable bandpass filters in this paper. Recently, the slot-line resonator has been extensively used to design the wideband bandpass filter [23–25]. It is very easy to use the slot line to implement a short-ended resonator. Like the conventional microstrip open-ended resonator [26, 27], the short-ended slot-line resonator can be used to enhance the diversity of filter design for meeting various requirements. For example, the uniplanar structure makes the proposed filter more applicable to MMIC/RFIC. With the use of voltage-wave analysis, it is obvious that the varactor should be located at the center of the slot-line resonator for tuning the fundamental frequency. In this case, the second harmonic remains unchanged. The theory will be verified by experiment. Next, by replacing the loading varactors with PIN diodes, a switchable bandpass filter is realized in which the attenuation level in the fundamental passband can be controlled. The demonstrated tunable and switchable bandpass filters are designed and fabricated on the substrate with a dielectric constant of 6.03 and a thickness of 0.82 mm. Their measured performance agrees well with the theoretical prediction.

2. CENTRALLY-LOADED SLOT-LINE RESONATOR

This section is divided into two parts to investigate the properties of the centrally-loaded slot-line resonator. Section 2.1 introduces the method of determining the location of the loading elements by using the voltage-wave analysis. Section 2.2 introduces the frequency response of the proposed resonator by using the odd- and even-mode analysis.

2.1. Voltage-wave Analysis

Figures 2(a) and (b) show the open- and short-circuit-ended half-wavelength resonators, the later represents the slot-line resonator shown in Fig. 1. According to the transmission line theory, electromagnetic field associated with the resonator can be expressed by voltage-wave functions. For lossless transmission line, the voltage on the line is [28]

$$V(l) = V_0 \left(e^{-j\beta l} + \Gamma e^{j\beta l} \right) \tag{1}$$

where $l \in [0, L]$, β is the propagation constant, and Γ is the reflection coefficient at the two ends of the resonator. For open-ended resonator, $\Gamma = 1$; while for short-circuit ended resonator, $\Gamma = -1$. Therefore, the normalized voltages at the fundamental frequency and second

harmonic of the open- and short-circuit ended resonators can be expressed as:

2.1.1. Open-ended Resonator

$$V_i(l) = \cos(i\beta_0 l) \tag{2}$$

2.1.2. Short-circuit Ended Resonator

$$V_i(l) = \sin(i\beta_0 l) \tag{3}$$

where $i = 1$ (fundamental frequency), or 2 (second harmonic), and β_0 is the propagation constant at the fundamental frequency. As can be seen from Fig. 2(a), by adding the varactors to the two ends of the open-ended resonator, the fundamental frequency and second harmonic are tuned simultaneously [6] because the voltages of the fundamental

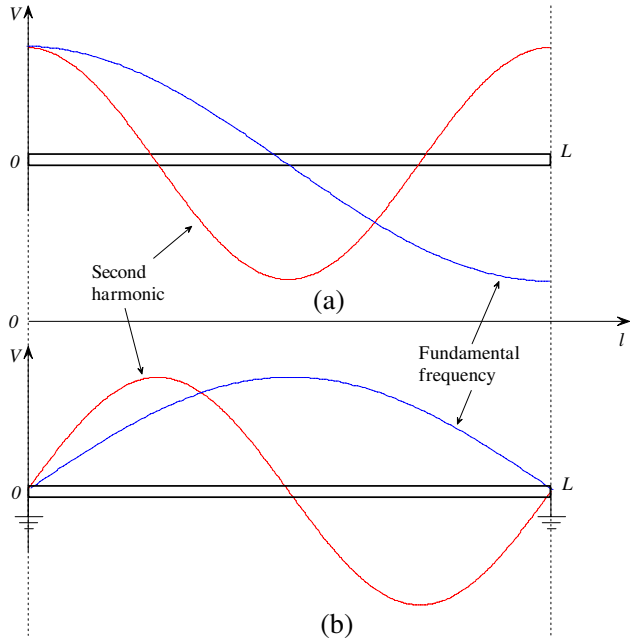

Figure 2. Normalized voltage wave along the half-wavelength resonators at fundamental frequency and second harmonic. (a) Open-ended resonator, (b) short-circuit ended resonator.

signal and second harmonic are both maximum at the two ends. It is always desirable to suppress the second harmonic in most microwave systems in that it is always twice of fundamental frequency. To reject the second harmonic, a resistor was added to the center of the open-ended resonator to absorb and then suppress the second harmonic while keeping fundamental frequency unchanged [29]. As a result, it can be concluded that in order to tune the fundamental frequency or second harmonic, the corresponding voltage at the connection point of the loading element should be maximum for good performance. If the voltage is zero, on the other hand, the loading element can be ignored.

As discussed, the loading capacitor C should be added to the center of the slot-line resonator shown in Fig. 3 to tune the fundamental frequency because the corresponding voltage at this point is maximum, as shown in Fig. 2(b). For the second harmonic, its voltage at the center of the resonator is zero, so the loading capacitor has no effect on the second harmonic. Therefore, the fundamental frequency can be tuned by changing C' value while the frequency of second harmonic keeps unchanged theoretically. This is desired in most applications because the second harmonic is no longer twice of the fundamental frequency when the loading C is not equal to zero. To calculate the resonant frequencies of the fundamental signal and second harmonic, the odd- and even-mode methods are used to analyze the centrally-loaded slot-line resonator. Different from the microstrip open-ended resonator, the excitation points of the odd- and even-modes are chosen at the two points, i.e., Feed 1 and 2, on the transmission line in that the two ends of the resonator are short-circuited. They are symmetric to the symmetrical line, as shown in Fig. 4(a).

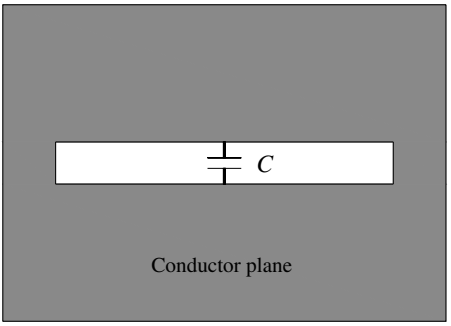

Figure 3. Centrally-loaded slot-line resonator.

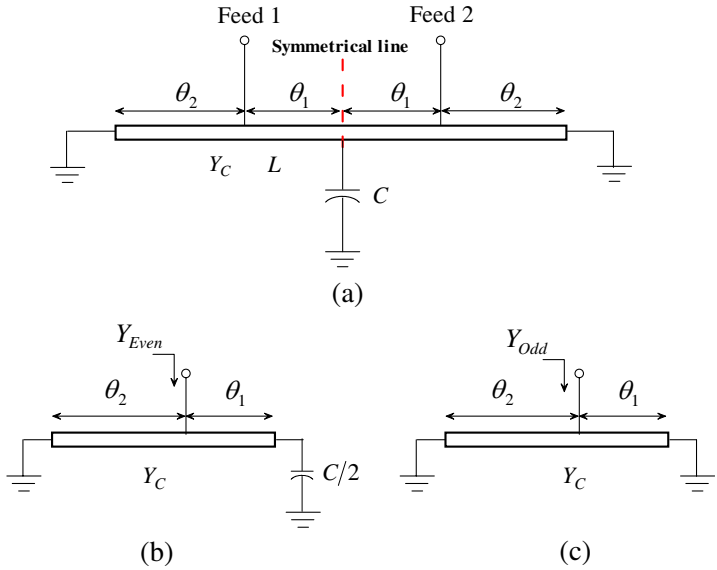

Figure 4. (a) Equivalent model of the centrally-loaded slot-line resonator, (b) even-mode equivalent circuit, and (c) odd-mode equivalent circuit.

2.2. Odd- and Even-mode Analysis

2.2.1. Even-mode Analysis

If even-mode excitation is applied to Feed 1 and 2 shown in Fig. 4(a), there is no current flowing through the center (symmetrical line) of the resonator. Therefore, we can symmetrically bisect the resonator and the loading capacitor to obtain the equivalent circuit shown in Fig. 4(b). The input admittance Y_{Even} is given by

$$Y_{Even} = -j\frac{Y_c}{\tan\theta_2} + Y_c\frac{jb + jY_c\tan\theta_1}{Y_c + j(jb)\tan\theta_1} \tag{4}$$

$$b = \frac{\omega C}{2} \tag{5}$$

where Y_c is the characteristic admittance of the transmission line, θ_i is the electrical length of the transmission line. Thus, the resonant condition is that the imaginary part of Y_{Even} is equal to 0, namely, $\mathrm{Im}\{\ Y_{Even}\} = 0$, resulting in

$$b(\tan\theta_1 + \tan\theta_2) + Y_c(\tan\theta_1\tan\theta_2 - 1) = 0 \tag{6a}$$

$$Y_c - b\tan\theta_1 \neq 0 \tag{6b}$$

From (6a),

$$b = \frac{Y_c(1 - \tan\theta_1 \tan\theta_2)}{\tan\theta_1 + \tan\theta_2} = \frac{Y_c}{\tan(\theta_1 + \theta_2)} \tag{7}$$

Thus, f_{Even} can be expressed as

$$f_{Even} = \frac{\left[\arctan(\frac{Y_c}{b}) + n\pi\right] \cdot c}{\pi L\sqrt{\varepsilon_{eff}}} \tag{8}$$

where $n = 0, 1, 2, 3, \ldots$, $n = 0$ is for the smallest length of resonator, c is the velocity of light in free space, ε_{eff} is the effective permittivity, and L is the length of the slot-line resonator. When $b = 0$, meaning no element is loaded, there is

$$f_{Even} = \frac{c}{2L\sqrt{\varepsilon_{eff}}} \tag{9}$$

It is found that the slot-line resonator is half-wavelength at the even-mode fundamental resonant frequency in the case of no loading capacitor. Therefore, the even-mode resonant frequency corresponds to the fundamental passband frequency of the bandpass filter designed using the proposed centrally-loaded slot-line resonator. When the loading capacitor is replaced by a varactor, b in (8) would be a function of voltage V, which is the reverse-biased voltage of the varactor. As a result, the even-mode resonant frequency can be tuned by varying the bias voltage of the varactor, as shown in Fig. 5.

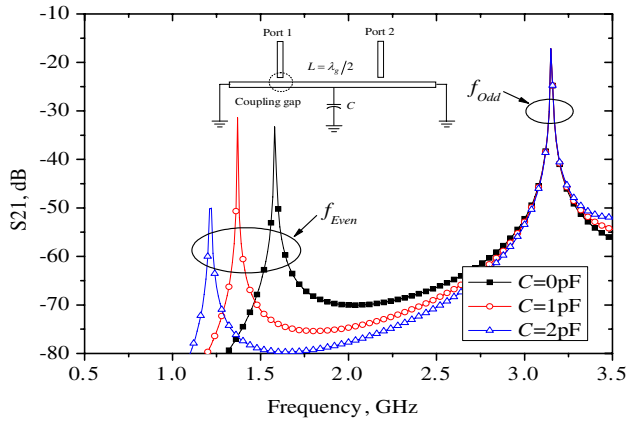

Figure 5. Simulated results of the centrally-loaded resonator in Fig. 4.

2.2.2. Odd-mode Analysis

If odd-mode excitation is applied to Feed 1 and 2 shown in Fig. 4(a), there is a voltage null at the center of the resonator. Therefore, the symmetrical line can be replaced by the short-circuited point in the equivalent circuit as shown in Fig. 4(c). Therefore, the loading capacitor has no effect on the odd-mode resonant frequency, and then can be ignored. The input admittance Y_{Odd} is given by

$$Y_{Odd} = -j\frac{Y_c}{\tan\theta_1} - j\frac{Y_c}{\tan\theta_2} \tag{10}$$

The resonant condition is that the imaginary part of Y_{Odd} is equal to 0, namely, $\mathrm{Im}\{Y_{Odd}\} = 0$, there must be

$$\theta_1 + \theta_2 = k\pi \tag{11a}$$

$$\theta_1 \text{ or } \theta_2 \neq \frac{(2k-1)\pi}{2} \tag{11b}$$

where $k = 1, 2, 3, \ldots, k = 1$ is for the smallest length of resonator. The resulted odd-mode resonant frequency can be obtained as follows

$$f_{Odd} = \frac{c}{L\sqrt{\varepsilon_{eff}}} \tag{12}$$

It is observed that the length L of the transmission line is one wavelength at the odd-mode resonant frequency; meanwhile, f_{Odd} is exact twice of f_{Even} when there is no loading element, as shown in Fig. 5. This feature is different from the open-ended half-wavelength resonator (where the odd-mode resonant frequency is just one half of the even-mode one [29]). Therefore, the odd-mode resonant frequency corresponds to the second harmonic of the bandpass filter designed using the centrally loaded slot-line resonator. From (12), it is determined by the length of transmission line and effective permittivity.

3. SLOT-LINE TUNABLE BANDPASS FILTER

3.1. Analysis and Design

Figure 6 shows the configuration of the proposed tunable bandpass filter designed using the centrally-loaded slot-line resonators, which are fed by 50 Ω CPW at the input and output. The interdigital structure is for enhancing the electric coupling between the CPW feed line and slot-line resonator [20]. A varactor and a capacitor C_1 in series are added to the slot-line resonator for tuning the fundamental frequency. Since the interdigital structures at the input and output enlarge the electrical length of the slot-line resonator, the location of the varactor

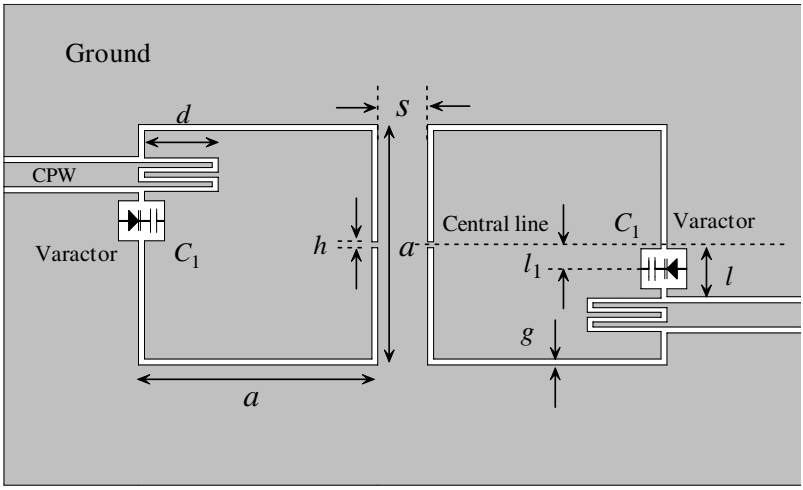

Parameters	a	d	g	h	l	s	l_1
Value (mm)	12	3.4	0.3	0.5	2.6	2.5	1.8

Figure 6. Tunable bandpass filter designed using the slot-line resonator.

should be optimized to be at the center of the slot-line resonator. Thus there is an offset l_1 between the connection point of the varactor and central line, as shown in Fig. 6. The bias voltage V_{bias} for the varactor is added to the point between the varactor and C_1. Thus, the total loading capacitor can be obtained

$$C_{total} = \frac{C_v C_1}{C_v + C_1} \tag{13}$$

where C_v represents the tunable capacitance of the varactor.

In this tunable filter design, the first step is to design a high performance bandpass filter without loading elements. The design principle is similar to that of the open-loop filter [30] by extracting external quality factor Q_e and coupling coefficient K for synthesis. The Q_e is calculated as

$$Q_e = \frac{f_0}{\Delta f_{\pm 90^\circ}} \tag{14}$$

where f_0 is the resonant frequency, and $\Delta f_{\pm 90^\circ}$ is the bandwidth about the resonant frequency over which the phase varies from -90° to $+90^\circ$. It is mainly determined by the tap position l in Fig. 6.

The K is calculated as

$$K = \frac{f_h^2 - f_l^2}{f_h^2 + f_l^2} \tag{15}$$

where f_h and f_l are the high and low resonant frequencies, respectively, as shown in Fig. 7. It is mainly controlled by the distance $s$between two slot-line resonators. As a result, by properly choosing the design parameters shown in Fig. 6, a good bandpass filter is simulated by using the HFSS software, as shown in Fig. 7.

After adding a varactor and a capacitor in series to the center of the resonator as shown in Fig. 6, the fundamental frequency varies with different V_{bias}. Based on (8), the fundamental frequency can be reduced by increasing the loading capacitor C_{total} in (13). Thus, the highest (lowest) tunable frequency is determined by the minimum (maximum) value of C_{total}. From (5) and (8), the tuning range of the fundamental frequency can be obtained in the case of the smallest length of the resonator ($n = 0$ in (8)).

$$\frac{\arctan\left(\frac{2Y_c}{\omega C_{total,\max}}\right) \cdot c}{\pi L\sqrt{\varepsilon_{eff}}} < f_{tunable} < \frac{\arctan\left(\frac{2Y_c}{\omega C_{total,\min}}\right) \cdot c}{\pi L\sqrt{\varepsilon_{eff}}} \tag{16}$$

Therefore, the tunable range of the fundamental frequency is determined by the available tuning range of C_{total}.

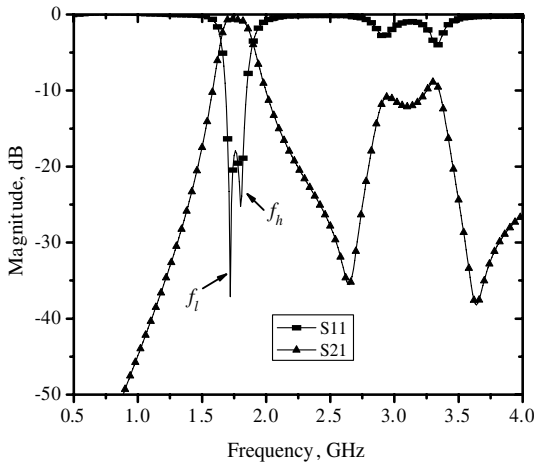

Figure 7. Simulated frequency response of the bandpass filter designed using the slot-line resonator without loading elements.

3.2. Results and Discussion

Figure 8 shows the implemented tunable bandpass filter using the proposed centrally-loaded slot-line resonator. The varactor used in this design is SMV1233-011LF from Skyworks Solutions Inc., Woburn, MA, with tunable capacitance from 0.84 to 5.08 pF over a 0–15 V bias range. Fig. 9 and Table 1 show the measured performance vs. different values of C_1 and reverse-biased voltage V_{bias} of the varactor. As V_{bias} is decreased from 15 V to 0 V, C_{total} in (13) increases, and then the center frequency of the fundamental passband reduces. From (13) and (16), if C_1 is large, the value of C_{total} has a wide tunable range, and then the fundamental passband frequency has a wide tuning range, which is verified by the experiments in Fig. 9 and Table 1. However, it is found that the insertion loss of the passband is increased as the passband frequency reduces. For example, the insertion loss is 5.25 dB at 1.02 GHz in the case of $V_{\text{bias}} = 0$ V and $C_1 = 3.3$ pF. This can be attributed to two factors: the first one is that the resistance of the varactor under low bias voltage is relative large; the second one is that the input matching deteriorates as the loading capacitor

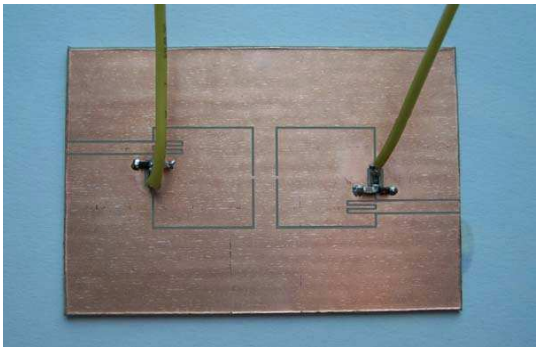

Figure 8. Fabricated tunable bandpass filter.

Table 1. Measured performance of the tunable bandpass filter with different.

C_1 (pF)	Tunable Frequency Range (GHz)	Tunable Bandwidth (%)	Insertion Loss (dB)
1.5	1.227–1.443	16.2	1.95–3.3
2.2	1.127–1.407	22.1	2.22–4.5
3.3	1.02–1.393	30.9	2.49–5.25

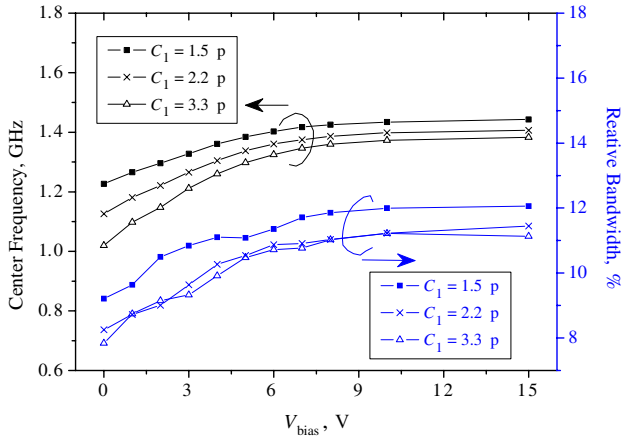

Figure 9. Measured center frequency and relative bandwidth of the fundamental passband of the tunable bandpass filter with different C_1 vs. the reverse-biased voltage V_{bias}.

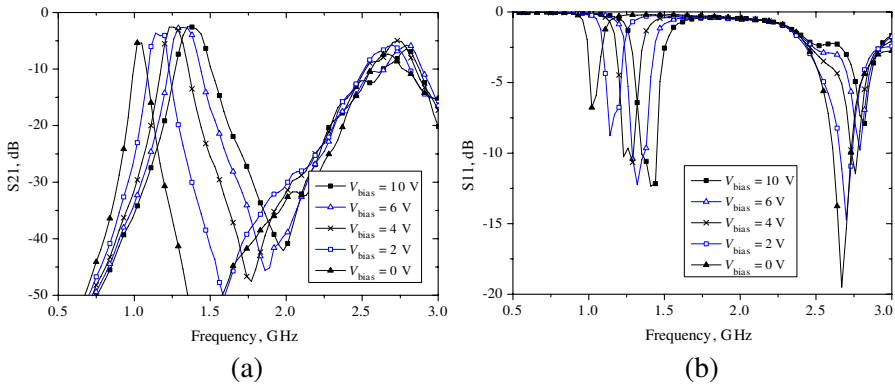

Figure 10. Measured S-parameters of the tunable bandpass filter with $C_1 = 3.3\,\text{pF}$, (a) S_{21}, (b) S_{11}.

C_{total} is increased. On the other hand, if C_1 is small, the tunable frequency range becomes a problematic issue. For example, when $C_1 = 1.5\,\text{pF}$, the tunable bandwidth is only 16.2%. Therefore, the trade-off between the tunable frequency bandwidth and insertion loss should be considered in this design.

Figure 10 shows the measured S-parameters of the tunable bandpass filter with $C_1 = 3.3\,\text{pF}$. The center frequency of the fundamental passband is reduced from 1.39 GHz to 1.02 GHz as V_{bias}

varies from 10 V to 0 V. The S-parameters keeps almost the same, which is not shown in Fig. 10, as V_{bias} varies from 15 V to 10 V because C_v changes very slightly in this biasing range. The 3 dB relative bandwidth variation of the passband is within $\pm 1.8\%$ (7.8%–11.14%), as shown in Fig. 9, and the relative bandwidth is enlarged as V_{bias} is increased. Meanwhile, as can be seen from Fig. 10, when the fundamental frequency is varied, the frequency of second harmonic almost maintains. It agrees well with the prediction in Section 2. The circuit size of the tunable bandpass filter is only $0.098\lambda_g \times 0.216\lambda_g$ at the highest tunable frequency of 1.393 GHz.

4. SLOT-LINE SWITCHABLE BANDPASS FILTER

For realizing a switchable bandpass filter, the varactors are replaced by the PIN diodes. The PIN diode in this design is SMP1345-079LF from Skyworks Solutions Inc., Woburn, MA. $C_1 = 82$ pF is used as a DC block. By tuning the bias voltage V_{bias} of the PIN diode, the fundamental passband can be switched either on or off. Fig. 11 shows the measured S-parameters under the situation of different V_{bias}. As can be seen, the center frequency of the fundamental passband drops down from 1.76 GHz (shown in Fig. 6) to 1.576 GHz due to the junction capacitance of 0.18 pF of the PIN diode and C_1 in series loaded at the center of the slot-line resonator. The insertion loss is 2.13 dB at 1.576 GHz when the PIN diode is off ($V_{\text{bias}} = 0$); while the attenuation reaches about 53.1 dB at 1.576 GHz and the attenuation level is more than 49 dB across the passband when the PIN diode is

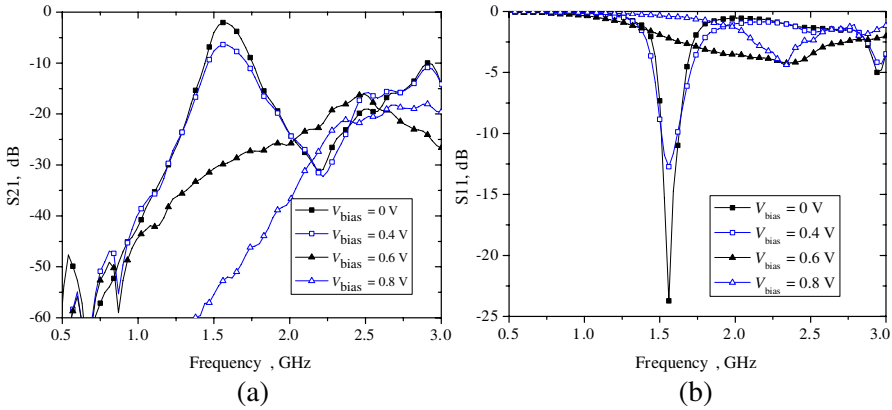

Figure 11. Measured S-parameters of the switchable bandpass filter, (a) S_{21}, (b) S_{11}.

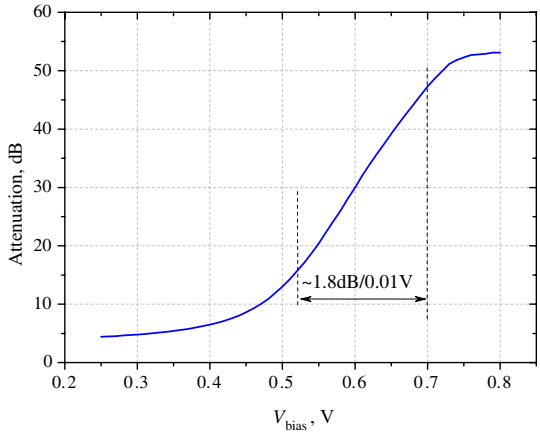

Figure 12. Attenuation level at the center frequency (1.576 GHz) of the passband vs. V_{bias} of the PIN diode.

on ($V_{\text{bias}} = 0.8\,\text{V}$). In the range of V_{bias} from 0.52 V to 0.7 V, the attenuation level at 1.576 GHz can be linearly tuned in dB, i.e., about 1.8 dB/0.01 V, shown in Fig. 12. The circuit size of the switchable bandpass filter is only about $0.108\lambda_g \times 0.236\lambda_g$ at the center frequency (1.576 GHz) of the passband.

5. CONCLUSION

In this paper, the centrally-loaded slot-line resonator has been investigated for the designs of the tunable and switchable bandpass filters. Both theoretical analysis and experimental results are given, showing good agreement. The expressions of the even- and odd-mode resonant frequencies of the centrally-loaded slot-line resonant are presented, which can be used as the design rules. In the tunable bandpass filter, by properly choosing the component values, the tunable range of the fundamental passband frequency is 30.9% with less than 5.25 dB insertion loss. For the switchable bandpass filter, the insertion loss is 2.13 dB at the center frequency of the passband and the attenuation is larger than 49 dB across the passband, respectively, when the centrally-loaded PIN diode is off and on. The uniplanar configuration of the proposed filter designed using the centrally loaded slot-line resonator should be useful to the MMIC and RFIC applications.

ACKNOWLEDGMENT

This work was supported by the National Natural Science Foundation of China under Grants 60901041, 60872002 and 61071086, and by the Natural Science Foundation of Jiangsu Province, China (Grant No. BK2010272).

REFERENCES

1. Ouyang, J., F. Yang, Z. P. Nie, and Z. Q. Zhao, "A novel frequency reconfigurable microstrip antenna for wideband application," *Journal of Electromagnetic Waves and Applications*, Vol. 22, No. 10, 1403–1410, 2008.
2. Monti, G., R. De Paolis, and L. Tarricone, "Design of a 3-state reconfigularable CRLH transmission line based on MEMS switches," *Progress In Electromagnetics Research*, Vol. 95, 283–297, 2009.
3. Vazquez, C., G. Hotopan, S. Ver Hoeye, M. Fernandez, L. F. Herran, and F. Las Heras, "Microstrip antenna design based on stacked patches for reconfigurable two dimensional planar array topologies," *Progress In Electromagnetics Research*, Vol. 97, 95–104, 2009.
4. Ourir, A., R. Abdeddaim, and J. de Rosny, "Tunable trapped mode in symmetric resonator designed for metamaterials," *Progress In Electromagnetics Research*, Vol. 101, 115–123, 2010.
5. Soliman, E. A., W. De Raedt, and G. A. E. Vandenbosch, "Reconfigurable slot antenna for polarization diversity," *Journal of Electromagnetic Waves and Applications*, Vol. 23, No. 7, 905–916, 2009.
6. Kim, J. and J. Choi, "Varactor-tuned microstrip bandpass filter with wide tuning range," *Microwave and Optical Technology Letters*, Vol. 50, 2574–2577, Oct. 2008.
7. Chang, K., S. Martin, F. Wang, and J. L. Klein, "On the study of microstrip ring and varactor-tuned ring circuits," *IEEE Transactions on Microwave Theory and Techniques*, Vol. 35, 1288–1295, Dec. 1987.
8. Torregrosa-Penalva, G., et al., "A simple method to design wide-band electronically tunable combline filters," *IEEE Transactions on Microwave Theory and Techniques*, Vol. 50, 172–177, Jan. 2002.
9. Masone, D. F. and J. C. Moreira, "Versatile microwave dual-band tunable resonator," *IET Microwaves, Antennas & Propagation*, Vol. 3, 71–76, 2009.

10. Sanchez-Renedo, M., et al., "Tunable combline filter with continuous control of center frequency and bandwidth," *IEEE Transactions on Microwave Theory and Techniques*, Vol. 53, 191–199, Jan. 2005.
11. Mohra, A. S. and O. F. Siddiqui, "Tunable bandpass filter based on capacitor-loaded metamaterial lines," *Electronics Letters*, Vol. 45, 470–472, Apr. 2009.
12. Abbaspour-Tamijani, A., L. Dussopt, and G. M. Rebeiz, "Miniature an tunable filters using MEMS capacitors," *IEEE Transactions on Microwave Theory and Techniques*, Vol. 51, 1878–1885, Jul. 2003.
13. Mercier, D., et al., "Millimeter-wave tune-all bandpass filters," *IEEE Transactions on Microwave Theory and Techniques*, Vol. 52, 1175–1181, Apr. 2004.
14. Park, S.-J., M. A. El-Tanani, I. Reines, and G. M. Rebeiz, "Low-loss 4-6-GHz tunable filter with 3-bit high-Q orthogonal bias RF-MEMS capacitance network," *IEEE Transactions on Microwave Theory and Techniques*, Vol. 56, 2348–2355, Oct. 2008.
15. Lugo, Jr., C. and J. Papapolymerou, "Electronic switchable bandpass filter using PIN diodes for wireless low cost system-on-a-package applications," *IEE Proc. — Microw. Antennas Propag.*, Vol. 151, 497–502, Dec. 2004.
16. Tu, W.-H. and K. Chang, "Piezoelectric transducer-controlled dual-mode dual-mode switchable bandpass filter," *IEEE Microwave and Wireless Components Letters*, Vol. 17, 199–201, Mar. 2007.
17. Chao, S.-F., C.-H. Wu, Z.-M. Tsai, H. Wang, and C. H. Chen, "Electronically switchable bandpass filters using loaded stepped-impedance resonators," *IEEE Transactions on Microwave Theory and Techniques*, Vol. 54, 4193–4201, Dec. 2006.
18. Dai, G. L., X. Y. Zhang, C. H. Chan, Q. Xue, and M. Y. Xia, "An investigation of open- and short-ended resonators and their applications to bandpass filters," *IEEE Transactions on Microwave Theory and Techniques*, Vol. 57, 2203–2210, Sep. 2009.
19. Mariani, E. A. and J. P. Agrios, "Slot-line filters and couplers," *IEEE Transactions on Microwave Theory and Techniques*, Vol. 18, 1089–1095, Dec. 1970.
20. Azadegan, R. and K. Sarabandi, "Miniature high-Q double-spiral slot-line resonator filters," *IEEE Transactions on Microwave Theory and Techniques*, Vol. 52, 1548–1557, May 2004.
21. Rahman, A. A., A. R. Ali, S. Amari, and A. S. Omar, "Compact

bandpass filter using defected ground structure (DGS) coupled resonators," *IEEE MTT-S Int. Dig.*, 1479–1482, 2005.

22. Deleniv, A., M. Gashinova, A. Eriksson, and A. Khalabuhov, "Novel band-pass filter utilizing S-shaped slot line resonators," *IEEE MTT-S Int. Dig.*, 1081–1084, 2003.
23. Mandal, M. K. and S. Sanyal, "Compact wide-band bandpass filter using microstrip to slotline broadside-coupling," *IEEE Microwave and Wireless Components Letters*, Vol. 17, 640–642, Sep. 2007.
24. Li, R., S. Sun, and L. Zhu, "Synthesis design of ultra-wideband bandpass filters with composite series and shunt stubs," *IEEE Transactions on Microwave Theory and Techniques*, Vol. 57, 684–692, Mar. 2009.
25. Mondal, P. and A. Chakrabarty, "Compact wideband bandpass filters with wide upper stopband," *IEEE Microwave and Wireless Components Letters*, Vol. 17, 31–33, Jan. 2007.
26. Velazquez-Ahumada, M. D. C., J. Martel, F. Medina, and F. Mesa, "Application of stub loaded folded stepped impedance resonators to dual band filter design," *Progress In Electromagnetics Research*, Vol. 102, 107–124, 2010.
27. Velazquez-Ahumada, M. D. C., J. Martel, F. Medina, and F. Mesa, "Design of a band-pass using stepped impedance resonators with floating conductors," *Progress In Electromagnetics Research*, Vol. 105, 31–48, 2010.
28. Pozar, D. M., *Microwave Engineering*, 2nd edition, Wiley, New York, 1998.
29. Zhang, X. Y. and Q. Xue, "Novel centrally loaded resonators and their applications to bandpass filters," *IEEE Transactions on Microwave Theory and Techniques*, Vol. 56, 913–921, Apr. 2008.
30. Hong, J.-S. and M. J. Lancaster, *Microstrip Filter for RF/Microwave Applications*, Wiley, New York, 2001.